

UDK 546.824, 612.086.3

Structural, Microstructural, Electrical Properties of Lanthanum doped-Bismuth Titanate Ceramics Prepared by Low Temperature Combustion Synthesis**Umar Al-Amani Azlan^{1*)}, Ahmad Fauzi Mohd Noor²**¹Faculty of Engineering Technology, Universiti Teknikal Malaysia Melaka, Hang Tuah Jaya, 76100 Durian Tunggal, Melaka, Malaysia²School of Material & Mineral Resources Engineering, Engineering Campus, Universiti Sains Malaysia, 14300, NibongTebal, Malaysia**Abstract:**

In this work, lanthanum doped-bismuth titanate with different contents were successfully prepared by low-temperature combustion synthesis, and subsequently, sintered at 1000 °C for 3 hours. Their structural, microstructural and electrical were systematically studied. It was found that the structural distortion of orthorhombic structure tends to transforms to a tetragonal with the increase in La content. This change is most probably due to relaxations of orthorhombic distortion and octahedral tilting because of the difference in the ionic radius of Bi³⁺ and La³⁺. Upon increasing of La content, the grain size remarkable decreases resulted in uniform grain size with better relative density. Thus, the electrical properties of La doping were greatly improved in comparison to pure sample.

Keywords: Bismuth titanate, Lanthanum, Structural, Microstructural, Electrical

1. Introduction

Lead-free ceramics have been widely studied for dielectric materials due to environmental friendly for their less toxicity. Among them, bismuth titanate, Bi₄Ti₃O₁₂ (BIT hereafter) has received a special attention for the fabrication of dielectric devices [1]. In general, BIT is a group of ferroelectric material with a high Curie temperature ($T_c = 675$ °C), high dielectric constant ($\epsilon_r = \sim 100$) and low dielectric loss ($\tan \delta = \sim 0.005$) [2]. However, several drawbacks of BIT limit its capability for advanced applications. It was reported that Bi ions, located at A-site in ABO₃ BIT structure, is known to be unstable due to easily volatile during sintering at temperature above 1000 °C [3]. Park et al. (1999) stated that the oxygen near the Bi ions is likely to be less stable due to the volatility of the Bi ions [4]. Thus, defects, such as bismuth vacancies (V_{Bi}^{'''}) and oxygen vacancies (V_O^{''}), could exist in the perovskite layers and act as a space charge. The presence of space charge implies that BIT has critical drawbacks such as high leakage current and domain pinning which then leads to low dielectric constant and high dielectric loss. Therefore, ion doping is a feasible method to improve the BIT structure, thus resulted in improved dielectric properties.

It was reported that the doping in BIT or ABO₃ can be performed on Bi ions (or A-site), Ti ions (or B-site) or both sites [5]. However, the doping of Bi ions at A-site is more

*) Corresponding author: umar@utem.edu.my

effective than Ti ions at B-site in enhancing the dielectric properties [6]. In addition, the doping on A-site is more suitable by rare-earths that possess similar ion valences. In principle, the role of doping is to displace the volatile Bi ions with dopant which in turn to suppress the Bi vacancies accompanied by oxygen vacancies. In other words, the space charge effect can be minimized and subsequently, resulted in high dielectric constant and low dielectric loss. On this basis, an attempt has been made to fabricate BIT with La doping to study their structural, morphological and electrical properties.

2. Experimental Procedure

In general, the preparation of BIT samples using low-temperature combustion synthesis was reported in earlier work [7]. Thus, the same technique was also used for BLaT preparation with different La content, ranging from 0.25 to 1.00 mol %. In this work, each pellet was sintered at 1000 °C for 3 hour in an electrical furnace. Characterizations and dielectric measurement on each sample were systematically carried out. Phase formation of the samples was analyzed by X-ray diffraction, XRD (Bruker D8-Discovery, Germany). Quantitative Rietveld refinement analysis was also examined by *X'pert High ScorePlus V. 2.2.5 program*. The structural changes observed in the formation of BIT from the combustion technique were carried out at room temperature using a Horiba Jobin-Yvon HR800UV Raman spectrometer in backscattering geometry. Additionally, Field emission scanning electron microscopy (FESEM) with model ZEISS SUPRA 35VP was used to investigate grain microstructure of the sintered samples. Determination on dielectric properties at different frequencies with an applied voltage of 500 mV was performed using LCR meter and dielectric test fixture (*Agilent 4284A*). This measurement was carried out at room temperature and the frequency range was set from 100 Hz to 1 MHz.

3. Results and Discussion

3.1. Structural analysis

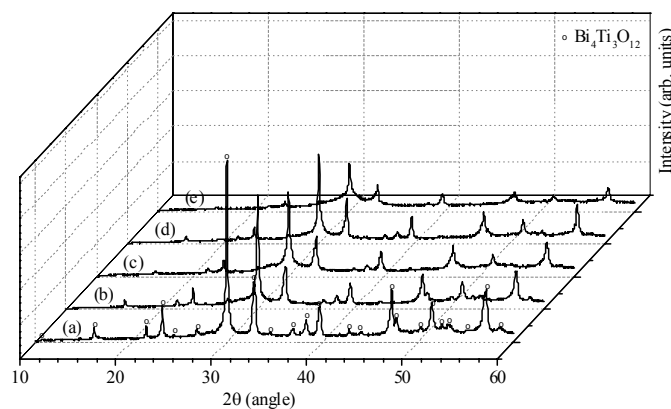


Fig. 1. XRD patterns of: (a) BIT, (b) BLaT25, (c) BLaT50, (d) BLaT75 and (e) BLaT100 powders.

Fig. 1 shows the XRD patterns of BLaT powders with different La content. For comparison, the XRD pattern of BIT powder was also included. The entire reflection peaks were analyzed using PDF 73-2181. As seen, the reflection peaks of BLaT powders agreed well with the standard file and no other phases were detected during the crystallization of

BLaT. This indicates that the BIT formation was successfully produced in BLaT regardless of La content. In addition to that, La^{3+} ion in the BLaT was well dissolved in the perovskite lattice. In the view of the ionic radius, it is obvious that La^{3+} ($r = 0.116$ nm) can occupy the A-site of Bi^{3+} ($r = 0.117$ nm), but it cannot enter into the B-site because the ionic radius of Ti^{4+} is rather small (0.0605 nm). This implies that La occupied Bi sites because the ionic radius of substituted is similar to that of host element. The doping effect clearly shows the change on peak intensity and peak width, as shown by the strong peak at $2\theta = 30^\circ$. As seen the intensity became less intense and the peak width became broader, indicating that the degree of crystallinity of BIT in substituted samples and their crystallite size decreased, respectively.

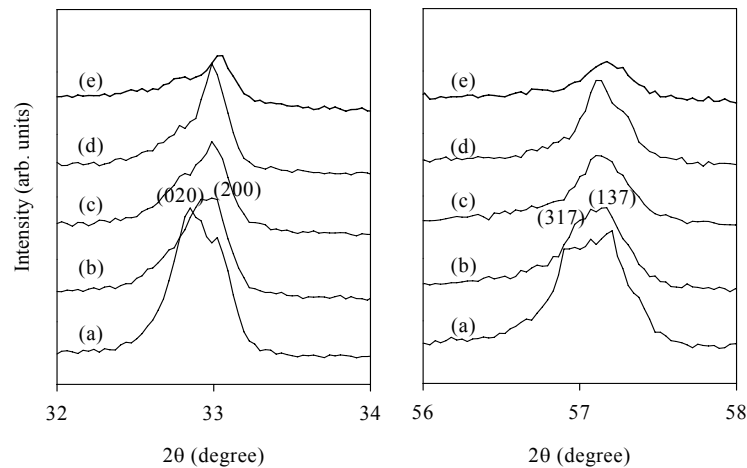


Fig. 2. Peak splitting of (020)/(200) and (317)/(137) reflections with different samples: (a) BIT, (b) BLaT25, (c) BLaT50, (d) BLaT75 and (e) BLaT100 powders.

Tab. I Refinement analysis of BLaT powders.

Samples	BIT	BLaT25	BLaT50	BLaT75	BLaT100
Refinement indexes					
Space group	<i>Fmmm</i>	<i>Fmmm</i>	<i>Fmmm</i>	<i>Fmmm</i>	<i>Fmmm</i>
R_{exp} , %	8.10	8.06	8.04	8.20	8.42
R_{wp} , %	14.19	15.06	17.01	17.03	16.32
GOF	3.06	3.46	4.49	4.28	3.76
S	1.75	1.86	2.12	2.07	1.94
Lattice parameters					
a , Å	5.4145	5.4206	5.4227	5.4239	5.4249
b , Å	5.4458	5.4384	5.4348	5.4296	5.4286
c , Å	32.7847	32.8047	32.8159	32.8245	32.8272
b/a	1.0058	1.0033	1.0022	1.0011	1.0007
Unit cell volume, Å ³	966.7	967.1	967.0	966.7	966.6
Density (g/cm ³)	8.05	8.05	8.05	8.06	8.09
Crystallite size, nm	49	36	10	8	3

Fig. 2 shows the peak splitting of (020)/(200) and (317)/(137) reflections in XRD patterns for the BLaT powders. The reflection of peaks splitting was gradually merged into a single peak as Lacontent increased above 0.5. This implies an increase in the symmetry of

crystal structure which is in agreement with the report by previous work [8]. It can be further confirmed by refinement analysis on the XRD pattern of BLaT.

The lattice parameters of BLaT powders were calculated according to the XRD patterns using the Rietveld refinement. The refinement results are summarized in Table I.

The R_{wp} of BLaT particularly at high La content showed a high value than that of BIT. The increase in R_{wp} can be explained by the change in peak characteristics i.e. intensity and width as a result of La doping. The increase S value for BLaT further supported the changes in the peak characteristic. The lattice parameters of BIT for a , b and c were calculated to be 5.4145, 5.4458 and 32.7847 Å, respectively, showing the formation of orthorhombic structure in the BIT lattice parameter. By La doping, the b -parameter approached gradually to the a -parameter with increasing La content. The convergence of the b -parameter to the a parameter imply to the structural distortion in the BLaT lattice. The structural distortion can be expressed by ratio of b/a , whereby the calculated ratio was almost to be 1, indicating that the orthorhombic structure tends to transforms to a tetragonal one with the increase in La content. The structure transformation can be explained by the increase of structural relaxation caused by La doping. The crystal structure transformation can be confirmed by the shrinkage of the unit cell volume as well as increased crystal density (Table I). Another notable effect is the reduction in crystallite size in substituted powders compared to that of BIT.

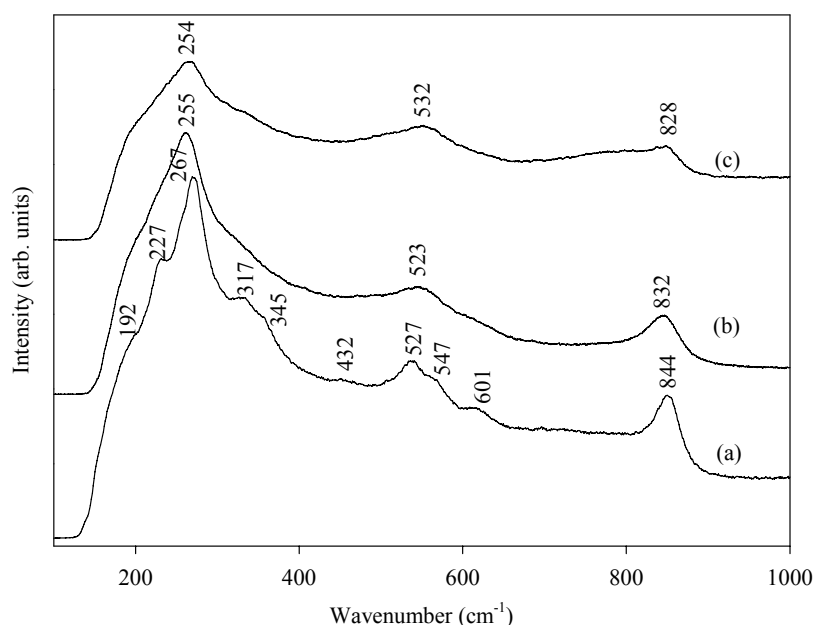


Fig. 3. Raman spectra of: (a) BIT, (b) BLaT25 and (c) BLaT75 powders.

Fig. 3 shows the Raman spectra of BIT and selected BLaT powders with different La content; 0.25 and 0.75. Ten Raman modes were detected at 192, 227, 267, 317, 345, 432, 527, 547, 601 and 844 cm^{-1} in the BIT spectrum. In comparison to the Raman spectrum of BIT, the number of Raman modes of BLaT was reduced to become three. The peak widths of 227, 317, 432 and 601 cm^{-1} increased with La content, and therefore identifying other modes of BIT with La doping was not feasible. It was clearly observed that the peak intensity decreased with increasing La contents from 0.25 to 0.75. It is believed to be associated with strong interactions between the ionic bonds; corresponding to the smaller ionic radius of La^{3+} (0.116 nm) compared with Bi^{3+} (0.117 nm). It was reported that the duplet peaks observed in Raman spectra tend to merge into single mode when the Bi ion is substituted by rare-earth elements. The result was also supported by other work, whereby they found in the case of Nd and Sm

doping [9]. In the present work, the duplet peaks at 227/267 and 527/547 cm^{-1} were found to merged into a single peak at 255 and 523 cm^{-1} for BLaT25 while 254 and 532 cm^{-1} for BLaT75. The main bands at 267, 527 and 844 cm^{-1} , which originated from TiO_6 octahedron, became weaken and broaden with increasing La content. These changes are most probably due to relaxations of orthorhombic distortion and octahedral tilting because of the difference in the ionic radius of Bi^{3+} and La^{3+} , which also supported by other researcher [10].

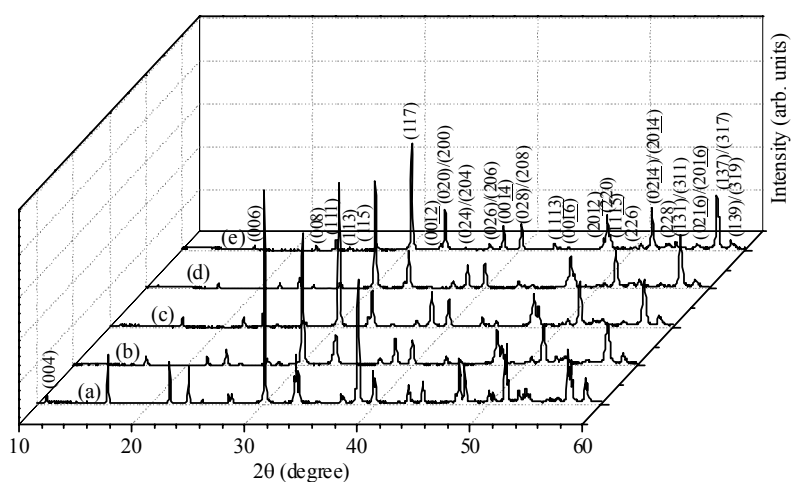


Fig. 4. XRD patterns of: (a) BIT, (b) BLaT25, (c) BLaT50, (d) BLaT75 and (e) BLaT100 ceramics.

The XRD patterns of BLaT with different La content at 1000 °C are illustrated in Fig. 4. It clearly indicates that the observed patterns are similar to the BIT perovskite structure, predominantly with (117) -axis orientation. The peak intensity and position are obviously different for BLaT as compared to BIT. As seen in Fig. 5, the intensity for (117) -reflection of substituted samples was reduced and the peak position was shifted to higher angles with increasing La content. The reduction of peak intensity due to low crystallinity of BLaT. The shifted in peak position designates the structural distortion, owing to the La doping for Bi ions in perovskite structure.

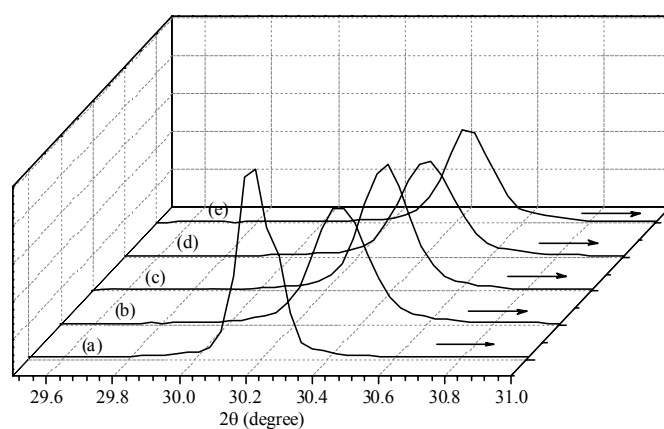


Fig. 5. (117) had shifted to high 2θ angle with increasing La content: (a) BIT, (b) BLaT25, (c) BLaT50, (d) BLaT75 and (e) BLaT100.

3.2. Microstructural observation

Fig. 6 shows the microstructures of BIT and BLaT ceramics with different La content. As seen, the morphology of BLaT25 (Fig. 6 (b)) is similar to BIT (Fig. 6 (a)), that consists of plate-like grains. However, the grain size remarkable decreases as compared to BIT.

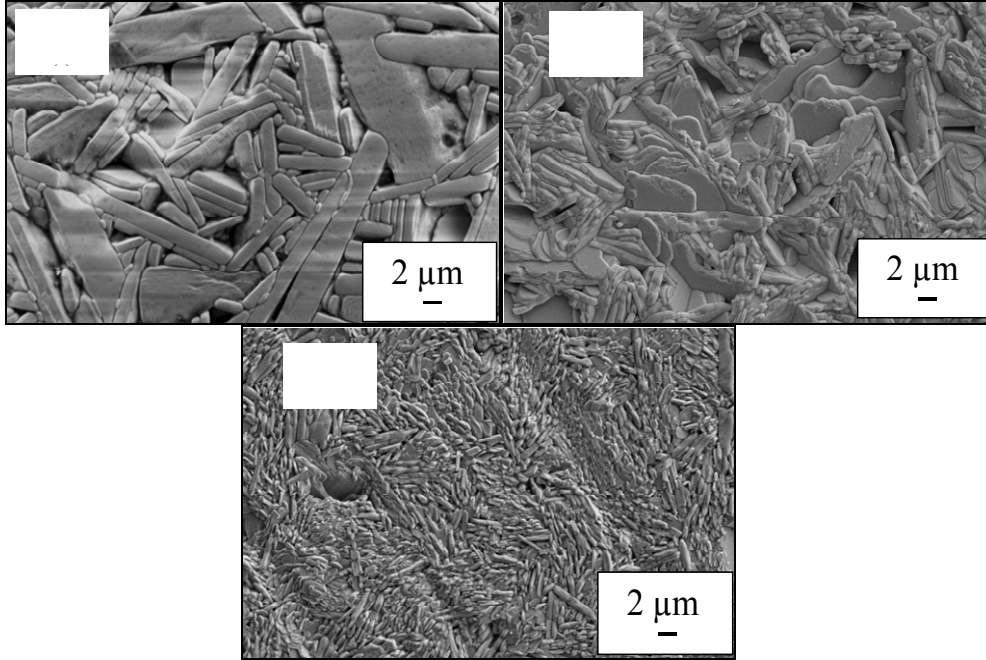


Fig. 6. Microstructure of (a) BIT, (b) BLaT25, (c) BLaT100 ceramics.

As discussed previously, BIT composed of plate-like grains with larger grain size in the range of 4 – 8 μm in length and 1.5 – 2 μm in width, which is about four times larger than BLaT100 (Fig. 6 (c)). It is also worth to note that high content of La (BLaT100) leads to formation of uniform grain size with better relative density (91 %). The reduced grain size in the range of 1.5 – 1.7 μm in length and 0.25 – 0.35 μm in width. This observation could be attributed to a greater suppression of the Bi^{3+} volatility by doping of low diffusivity of La^{3+} , which eventually inhibits the grain growth.

3.3. Electrical properties

Fig. 7 shows the dielectric constant (ϵ_r) of BIT and BLaT ceramics measured from 100 Hz to 1 MHz at room temperature. It shows that ϵ_r of substituted samples decreased with increasing frequency particularly from 100 Hz to 50 kHz and subsequently remains constant. Besides that, there is a significant improvement in ϵ_r with incorporation of La into BIT. The improved ϵ_r in substituted samples is clearly shown in the inset Fig. 7. The results can be explained by several factors. As shown in refinement data in Table I, the lattice parameters and cell volume in substituted samples changed due to the difference in the ionic radius within La^{3+} and Bi^{3+} . The increase in the lattice parameters result in large octahedral volume and hence increase in ϵ_r . Besides that, the increase in ϵ_r of BLaT samples can be ascribed to the improved microstructures. The controlled microstructure with small grain size eventually contributed to the formation of the 90° domains orientation, thus resulting in better ϵ_r of ceramics.

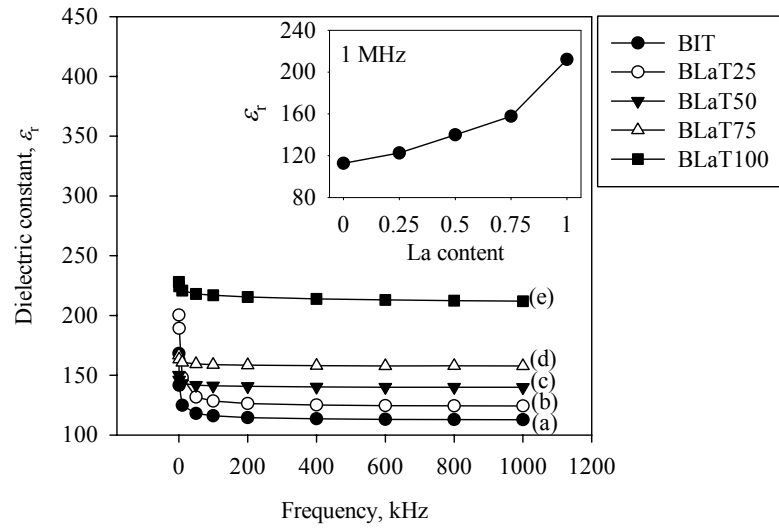


Fig. 7. Dielectric constant, ϵ_r of: (a) BIT, (b) BLaT25, (c) BLaT50, (d) BLaT75 and (e) BLaT100 measured at different frequencies. Inset showing the dielectric constant at 1 MHz.

Fig. 8 shows the dielectric loss ($\tan \delta$) of BIT and BLaT ceramics with different La content as a function of frequency. As seen, the dielectric loss is dependent on frequency and La content. The dielectric loss was significantly decreased with increasing frequency for the entire samples. The loss in ceramics is caused by space charge and domain wall relaxation, as reported by [11-12].

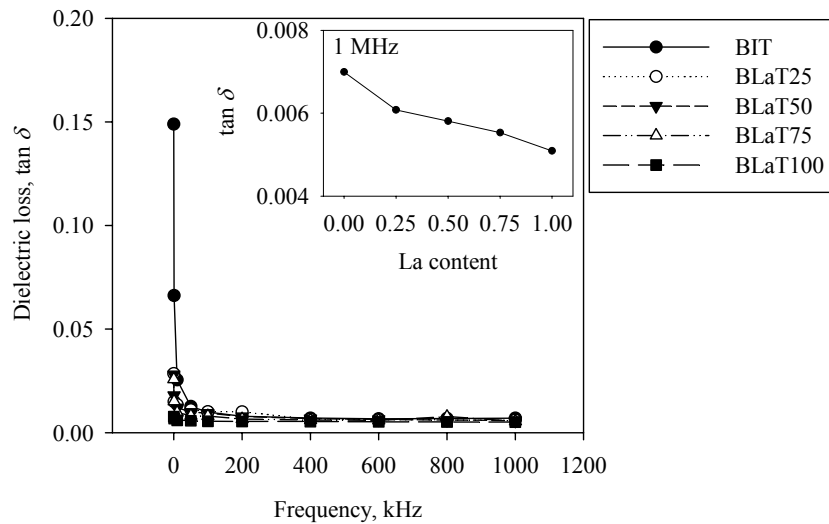


Fig. 8. Dielectric loss, $\tan \delta$ of BIT and BLaT ceramics as a function of frequency.

Atomic, ionic and space charge polarization are the main contributors to dielectric loss in ceramics. Response frequencies for atomic and ionic polarization are 10^{15} and 10^{13} Hz, respectively. Space charge polarization has a response frequency of 100 Hz as stated by [13]. At high frequency, space charge polarization does not exist and hence $\tan \delta$ decreases with increasing frequency. The presence of oxygen vacancies which acts as space charge, could also contribute to the electronic polarization which can be related to $\tan \delta$. As seen by inset in Fig. 8, La doping effectively reduces the concentration of oxygen in BLaT samples. This also

imply to low $\tan\delta$ in substituted samples. Again, the improvement of $\tan\delta$ dispersion of substituted samples as a function of frequency and La content is due to fewer defects in perovskite structure such as oxygen vacancies and bismuth vacancies.

4. Conclusion

The formation of single phase BIT in BLAT regardless of La content was successfully produced after synthesis and sintering. Their structural analyses with La doping were systematically studied by XRD, Refinement and Raman, where by the change of peak characteristics were clearly observed in La doping. On the microstructural analysis, the uniform grain size with better relative density was obtained at high La content. As a result, the improved electrical properties were then achieved with La doping samples.

Acknowledgment

Special thanks to Universiti Teknikal Malaysia Melaka (FRGS/1/2014/TK04/FTK/02/F00207) for financial support.

5. References

1. Z. Lazarević, B. D. Stojanović, J. A. Varela, Sci. Sinter., 37 (2005) 199.
2. J. O. Herrera Robles, C. A. Rodríguez González, S. D. De La Torre, L. E. Fuentes Cobas, P. E. García Casillas, H. Camacho Montes, J. Alloy Compd., 536 (2012) 511.
3. P.-H. Xiang, Y. Kinemuchi, T. Nagaoka, K. Watari, Mater. Lett., 59 (2005) 3590.
4. B. H. Park, B. S. Kang, S. D. Bu, T. W. Noh, J. Lee, W. Jo, Nature, 401 (1999) 682.
5. U. Al-Amani Azlan, S. Sreekantan, M. N. Ahmad Fauzi, K. A. Razak, Bismuth: Characteristics, Production and Applications, Nova Science Publishers, Inc. New York, 123 (2012).
6. C. M. Wang, L. Zhao, J. F. Wang, L. M. Zheng, J. Du, M. L. Zhao, C. L. Wang, Mat. Sci. Eng. B-Solid, 163 (2009) 179.
7. U. Al-Amani, S. Sreekantan, M. N. Ahmad Fauzi, A. R. Khairunisak, K. Warapong, Sci. Sinter., 44 (2012) 211.
8. Y. M. Kan, G. J. Zhang, P. L. Wang, Y. B. Cheng, J. Eur. Ceram. Soc., 28 (2008) 1641.
9. D. Wu, Y. Deng, C. L. Mak, K. H. Wong, A. D. Li, M. S. Zhang, N. B. Ming, Appl. Phys. A-Mater., 80 (2005) 607.
10. C. V. Kannan, Z. X. Cheng, H. Kimura, K. Shimamura, A. Miyazaki, K. Kitamura, J. Cryst. Growth, 292 (2006) 485.
11. N. V. Prasad, S. N. Babu, A. Siddeshwar, G. Prasad, G. S. Kumar, Ceram. Int., 35 (2009) 1057.
12. J. Y. Yi, J. K. Lee, J. Phys. D: Appl. Phys., 44 (2011) 1.
13. A. Kumar, K. Yadav, Physica B, 405 (2010) 4650.

Садржај: У овом раду, бизмут титанат са различитим садржајем La је успешно припремљен употребом ниско-температурске синтезе сагоревањем и потом синтеровањем на 1000 °C током 3 сата. Структурна, микроструктурна и електрична

својства су синстематично проучавана. Нађено је да орторомбична структура тежи трансформацији у тетрагоналну са повећањем садржаја лантана. Ова промена настаје услед релаксације орторомбичне структуре и кривљења октаедара услед разлике у јонским радијусима Bi^{3+} и La^{3+} . Услед повећања садржаја лантана, значајно је смањена величина зрна резултујући униформној величини зрна и већој релативној густини. Исто тако, електрична својства су значајно побољшана са додатком лантана, а у поређењу са чистим недопираним узорцима.

Кључне речи: бизмут титанат, лантан, структура, микроструктура, електрична својства.

© 2016 Authors. Published by the International Institute for the Science of Sintering. This article is an open access article distributed under the terms and conditions of the Creative Commons — Attribution 4.0 International license (<https://creativecommons.org/licenses/by/4.0/>).

